



HAL
open science

Dynamic magnetostriction for antiferromagnets

Thomas Nussle, Pascal Thibaudeau, Stam Nicolis

► **To cite this version:**

Thomas Nussle, Pascal Thibaudeau, Stam Nicolis. Dynamic magnetostriction for antiferromagnets. Physical Review B, 2019, 100, pp.214428. cea-02168016

HAL Id: cea-02168016

<https://cea.hal.science/cea-02168016>

Submitted on 28 Jun 2019

HAL is a multi-disciplinary open access archive for the deposit and dissemination of scientific research documents, whether they are published or not. The documents may come from teaching and research institutions in France or abroad, or from public or private research centers.

L'archive ouverte pluridisciplinaire **HAL**, est destinée au dépôt et à la diffusion de documents scientifiques de niveau recherche, publiés ou non, émanant des établissements d'enseignement et de recherche français ou étrangers, des laboratoires publics ou privés.

Dynamic magnetostriction for antiferromagnets

Thomas Nussle*

*CEA DAM/Le Ripault, BP 16, F-37260, Monts, FRANCE and
Institut Denis Poisson, Université de Tours, Université d'Orléans,
CNRS (UMR7013), Parc de Grandmont, F-37200, Tours, FRANCE*

Pascal Thibaudeau†

CEA DAM/Le Ripault, BP 16, F-37260, Monts, FRANCE

Stam Nicolis‡

*Institut Denis Poisson, Université de Tours, Université d'Orléans,
CNRS (UMR7013), Parc de Grandmont, F-37200, Tours, FRANCE*

In this paper we propose a Hamiltonian framework for the dynamics of magnetic moments, in interaction with an elastic medium, that can take into account the dynamics in phase space of the variables that describe the magnetic moments in a consistent way. While such a description involves describing the magnetic moments as bilinears of anticommuting variables that are their own conjugates, we show how it is possible to avoid having to deal directly with the anticommuting variables themselves, only using them to deduce non-trivial constraints on the magnetoelastic couplings. We construct the appropriate Poisson bracket and a geometric integration scheme, that is symplectic in the extended phase space and that allows us to study the switching properties of the magnetization, that are relevant for applications, for the case of a toy model for antiferromagnetic NiO, under external stresses.

I. INTRODUCTION

The interest in precision devices based on voltage-controlled ferromagnetism is focusing the attention of theory and applications towards developing materials with strong intrinsic ferroelectric and/or ferromagnetic response; what is of particular interest is that these can be produced through an appropriate spin-lattice coupling, that can be controlled, experimentally, in real materials¹. What is, particularly, fascinating is that such couplings lead to novel situations, where it is possible to control the magnetic properties through electric fields and vice versa. This class of phenomena is known under the name of *magneto-electric effects*, and there are several ways in which such magneto-electric effects can be engineered in magnetic materials.

For instance, antiferromagnets (AFs) are the magnetically ordered materials which could be the most suitable for realizing the fastest spintronic devices². Recent progress in describing spin transport and spin-transfer torque (STT) effect in such AF devices open a route towards multilevel memory devices with switching speeds, that could exceed those of devices made of ferromagnetic materials and semiconductors³. Moreover reversible strain-induced magnetization switching in ferromagnetic materials has been reported that also allows the design of a rewritable, non-volatile, non-toggle and extremely low energy straintronic memory⁴. Recently a piezoelectric, strain-controlled AF memory, insensitive to magnetic fields, has been tested, as an example of controlling magnetism by electric fields in multiferroic heterostructures⁵.

However a complete theoretical description of all such phenomena is, still, very much, work in progress, since, at

the scales, that are relevant, it is not possible to separate the scales of the magnetic, electric and elastic responses—all must be treated together.

It is, indeed, noteworthy that no direct local coupling between electromagnetic field components is allowed in the vacuum; the magnetic response to an electric field is necessarily mediated by atomic position arrangements of magnetic moments, in a potentially ionic environment, that produce non-local mechanical strains in response^{6,7}. These illustrate the different physical origins of the spin-lattice coupling—in particular, either as emerging from a macroscopic magnetostriction⁸ or, at a more microscopic scale, from the usual spin-orbit coupling in materials^{9,10}, however, considerably enhanced from the effects of magneto-elastic effects.

The idea to couple the dynamics of mechanical and magnetic degrees of freedom in matter is, of course, not new, and many strategies to produce a general conceptual framework have been explored to date, covering a quite broad spectrum of approaches and applications. Illustrations of the interplay between magnetism and mechanical elasticity in matter are so diverse that a large variety of techniques and ideas have been developed, with just as many different motivations¹¹.

It is, also, relevant to mention magnetic molecular dynamics¹², which emerges from the fluid mechanics framework and assumes position-dependent magnetic interactions between particles, under a tight time-evolution of their own spins. From granular fields theories, apparently radically different perspectives can be gleaned, such as Edwards field theory¹³, which focuses on the long distance correlations between mechanical stresses in large systems, assuming material properties as point-particle stress distributions and interactions.

A common focus of all these approaches is, however, not at all obvious.

In addition, until recently, sufficient experimental control over the materials that could be candidates for realizing such effects in practice was not that common. It is this last fact that has changed in recent years. This, in turn, has made the call for theoretical tools more urgent. While it has become much easier to develop computational strategies, thanks to the progress in hardware and software, theoretical concepts have tended to lag behind the events.

Magneto-elastic phenomena are, typically, viewed from the continuum mechanics perspective where the magnetic properties of materials are incorporated into constitutive nonlinear laws of electro-conductive bodies¹⁴. Even if multiscale models have been investigated for magneto-elastic couplings¹⁵, with good experimental comparison for single crystals and polycrystalline samples¹⁶, localization and homogenization procedures are still the mainstays for deducing the constitutive laws for polycrystalline media. Homogenization methods for multiscale mechanics assume the existence of well-separated scales and different relations among length scales, that lead to different effective equations, which, in turn, represent the corresponding different physical effects, appropriate at each scale¹⁷.

Renormalization group ideas, of course, are instrumental in providing a description of how the dynamics depends on the scale; what has been lacking, to date, is a unified construction of the dynamics of elastic and spin degrees of freedom, within a common Hamiltonian approach, at any particular scale. In particular, what has, curiously, not been fully exploited is the resolution of the constraints, that the spin degrees of freedom are subject to, since they are their own canonically conjugate variables, as their equations of motion are first order. This means that they can be most usefully expressed as multilinear combinations of *anticommuting* variables. As we shall see, this can lead to useful insights, in practice, about the dynamics of the coupled system.

While the generalization of the canonical formalism, that incorporates the constraints implied by spin degrees of freedom has been worked out a long time ago¹⁸⁻²⁰, it has not been applied to concrete situations of physical interest, simply because these, up to now, were not of practical relevance.

In the present paper we fill this gap. We provide a complete description of the combined dynamics of the elastic and of the spin degrees of freedom in phase space and show how the anticommuting nature of the spin degrees of freedom can be indirectly tested. It is the refined control over these that is the particular novelty of our approach. In future work we shall show how to incorporate stochastic effects, due to noise and/or disorder.

We consider our medium as the limit of a large number of sites; to each site is assigned a spin and a local mechanical deformation variable. We deduce the corresponding equations of motion from a formalism, that

treats mechanical and spin degrees of freedom in a unified way and study the dynamics of this system, comparing it to previous studies for the purely magnetic part²¹ and for the magneto-elastically coupled system²². We stress that the novelty of the current approach lies, on the one hand, in dealing with a consistently closed system; on the other hand, in being able to extract the information that the commuting degrees of freedom, that describe the spins are, in fact, composite operators of anticommuting fields.

The paper is organized as follows, in section II we construct a classical Hamiltonian for the mechanical, and the spin degrees of freedom and discuss their couplings. In section III, we introduce a particular Poisson bracket, which allows us to obtain the equations of motion for the time-evolution of all the dynamical variables. These are, then solved, in section IV using a symplectic integration scheme. Special attention is devoted to the stability analysis of the schemes and to the order of the different symplectic operators. This analysis is presented in the appendix. Finally in section V we illustrate the formalism for the case of a simple toy model for NiO, consisting of two spins, interacting through antiferromagnetic exchange, and subject to an external SST, as well as under an external stress.

II. THE HAMILTONIAN

In this section we propose a Hamiltonian for the combined system of elastic and spin degrees of freedom. These parts have, of course, been considered before⁸, so we shall review the salient features, before introducing our approach.

The starting point for the elastic degrees of freedom is the framework of mechanics for elastic solids, within the régime of the approximation of small deformations, supplemented by the assumption of perfect mechanical micro-reversibility²³. These statements imply that an elastic material is characterized by a collection of N time-dependant elastic deformations, which are described by a set of symmetric Cauchy strain tensors $\epsilon_{IJ}^i(t)$ where I, J are spatial indices, ranging from 1 to 3, and assigned to each lattice site, $i \in \{1..N\}$, of the material. At equilibrium, each of these variables is independent of time and we assume that such a state not only exists, but can be relevant for the time scales of interest.

The total internal energy of this system can be described in terms of the interactions between these variables, that take into account the elastic mechanical part in the most general form^{24,25}; to lowest, non-trivial, i.e. quadratic, order, we have

$$\frac{\mathcal{H}_{\text{mech}}}{V_0} = \frac{1}{2} \sum_{i=1}^N C_{IJKL}^i \epsilon_{IJ}^i(t) \epsilon_{KL}^i(t), \quad (1)$$

where an implicit sum on the repeated space indices is understood and where C_{IJKL}^i are the elastic constants

with V_0 as the reference volume.

In this expression we have assumed that the different sites of the material do not interact through elastic deformations (they will only interact through spin exchange forces, to be spelled out below).

For a homogeneous material, these elastic constants can be expressed in terms of the two Lamé parameters²³, designated, as usual, by (λ, μ) , in Cartesian coordinates as follows:

$$C_{IJKL} = \lambda \delta_{IJ} \delta_{KL} + \mu (\delta_{IK} \delta_{JL} + \delta_{IL} \delta_{JK}) \quad (2)$$

This mechanical system can be excited by an external stress σ_{IJ}^{ext} , through the coupling

$$\frac{\mathcal{H}_{\text{ext}}}{V_0} = - \sum_{i=1}^N \sigma_{IJ}^{\text{ext}} \epsilon_{JI}^i \quad (3)$$

While this stress can be, in general, a time- and space-dependent quantity, it is, nonetheless, assumed to be uniform over the sites of the material.

Now we introduce the magnetic degrees of freedom, noted $S_I^i(t)$ and describe how their dynamics affects the mechanical degrees of freedom, through the so-called magnetoelastic coupling. The contribution of the magnetoelastic coupling to the Hamiltonian can be deduced by assuming (global) Galilean invariance on the one hand and imposing invariance under the symmetries of the point group²⁶ on the other. For an isotropic medium, these requirements lead to the expressions for the total energy and the total magnetization²⁷. The total internal energy is, thus, a sum over the lattice $U(\epsilon_{IJ}^i, S_I^i)$ ²⁸.

Consequently, in the approximation of small deformations, the expansion of the magnetoelastic coupling energy will contain even powers of the magnetization S^i . It will, however, contain all powers of the strain tensor, ϵ .

The linear part in ϵ_{IJ}^i defines the linear, or first-order, magnetoelastic coupling, which is responsible for the magnetostriction, while the quadratic terms in ϵ_{IJ}^i define the second-order magnetoelastic coupling, that are responsible for “nonlinear response” in the elastic properties of magnetic media, that have been, also, identified as describing “anomalous effects”.

Higher order terms are, usually, ignored, since their coefficients are assumed to be much smaller than the lower order terms, already discussed.

Therefore, the contribution to the Hamiltonian of the magnetoelastic coupling can be written as

$$\begin{aligned} \mathcal{H}_{\text{ME}} = & \sum_{i,j=1}^N B_{IJKL}^{(1)i,j} \epsilon_{IJ}^i(t) S_K^i(t) S_L^j(t) \\ & + B_{IJKLMN}^{(2)i,j} \epsilon_{IJ}^i(t) \epsilon_{KL}^j(t) S_M^i(t) S_N^j(t) + \dots \quad (4) \end{aligned}$$

If one compares the last term of equation (4) with equation (1), it is easy to see that a pair of effective elastic

constants can be introduced that depends on the value of the spins on each site, i.e.

$$C_{IJKL}^{\text{eff},i,j} \equiv C_{IJKL}^{ij} + \frac{1}{V_0} B_{IJKLMN}^{(2)i,j} S_M^i(t) S_N^j(t). \quad (5)$$

This allows a possible interpretation of the “anomalous” temperature dependence in the elastic constants in iron single crystals as resulting from the competition between spin ordering and diffusion effects²⁹.

In Appendix A we recall that the most effective “classically equivalent description” of the spin degree of freedom, that can capture such effects is not through the, commuting, variables \mathbf{S} but their, anticommuting, “Doppelgänger” $\boldsymbol{\xi}$, related to the S_I^i through

$$S_I^i \equiv -\frac{i}{2} \epsilon_{IJK} \xi_J^i \xi_K^i. \quad (6)$$

The $\boldsymbol{\xi}$ can be identified with Majorana fermions, which have found many applications recently in condensed matter systems^{30,31}, where new methods for controlling spin degrees of freedom have been developed.

It is interesting to remark that the anticommuting variables, ξ_k^i are not Grassmann variables, satisfying $\{\xi_I^i, \xi_J^j\} = 0$; but, rather, $\{\xi_I^i, \xi_J^i\} = \delta^{ij} \delta_{IJ}$, i.e. that the ξ_I^i generate a Clifford algebra on each site³². It is in this way that the S_I^i , defined through eq. (6), satisfy the angular momentum algebra.

If one were tempted to simply replace \mathbf{S} by $\boldsymbol{\xi}$ in eq.(4), it is interesting to remark that, for $N = 1$, and because of the symmetries of $B^{(1)}$, $\mathcal{H}_{\text{ME}} = 0$, which implies that the dynamics as it is cannot be encoded by this Hamiltonian.

On the other hand, this allows us to understand the constraints on the allowed terms in the true Hamiltonian. They must, necessarily, involve more than one spins. Indeed, we can construct expressions that are multi-linear combinations of the S_I^i on different sites, potentially, up to order N , the number of sites, since no two identical ξ_I^i variables occur in the same monomial. This is, therefore, a nice way of automatically organizing the multi-spin terms of the Hamiltonian.

In the formalism of Atomistic Spin Dynamics, since the magnetic moments are localized^{33,34}, it is customary to consider spatial averages, around each site, defining an effective macroscopic localized spin

$$S_I^{\text{eff}} = \langle S_I^i \rangle_i \quad (7)$$

which implies that multi-linear expressions, $S_I S_J$ no longer vanish identically, as was imposed by the anticommuting nature of $\boldsymbol{\xi}$ before. We can, thus, understand the relevance of this averaging procedure, in terms of the description of the spin degrees of freedom in terms of the anticommuting variables.

The microscopic mechanism behind equation (4) has been advocated a long time ago³⁵⁻³⁷, as a model for a two-body interaction, that is itself a pedagogical version of the quantum theory of interacting magnons and phonons³⁸. In eq. (4) what has been left unspecified are

the properties of the tensor $B^{(1)}$ under exchange of the indices i and j , that label the sites. What is customary is to assume that $B^{(1)}$, in fact, does not depend on i and j at all—it is homogeneous across the material. By stopping the expansion at first order in the mechanical deformation in (4) and assuming homogeneity in the material, we, therefore, end up with the following expression

$$\mathcal{H}_{\text{ME}} = B_{IJKL}^{(1)} \epsilon_{IJ}(t) S_K(t) S_L(t). \quad (8)$$

In summary, the microscopic theory underlying Eq.(8) describes the interaction of three particles, two of which are spin states, and one is the state of the elastic deformation. However the spin states, are, in fact, bound states of more “fundamental” entities, the anticommuting ξ . $B^{(1)}$ can then be interpreted as the vertex of this interaction, that describes a spinning particle, that does not directly interact with itself—since any such interaction is inconsistent with the fact that the ξ anticommute. Such a self-interaction can, however, appear on larger scales, when spatial averages can become meaningful for describing the spin degrees of freedom.

In conclusion to this section, the Hamiltonian we have constructed describes the interaction of magnetic moments through their embedding within an elastic medium. What remains to be done is to define the Poisson brackets, that can take into account the evolution in phase space of commuting, as well as anticommuting degrees of freedom. Indeed, the construction procedure for commuting canonical variables is well known, however, including anticommuting variables in a unified way has remained a rather esoteric subject—known in theory^{18–20}, not, however, implemented, in practice.

In the following section, we shall construct the equations of motion in the phase space of the elastic and the spinning degrees of freedom, that implements these ideas in practice.

In order to work directly with the anticommuting variables themselves, in combination with the mechanical degrees of freedom requires implementing a “graded Poisson bracket”; one way to do this is discussed in Appendix A.

III. THE POISSON BRACKETS AND THE EQUATIONS OF MOTION

To deduce from the Hamiltonian, discussed in the previous section, the equations of motion, we must define the appropriate pairs of canonically conjugate variables and consequently their Poisson bracket.

First we recognize that ϵ acts as a tensor and one can understand the definition of the Poisson bracket of rank-2 symmetric tensors as an application of the DeDonder-Weyl covariant hamiltonian formulation of field theory³⁹. Although the context is different, the ADM procedure in general relativity also provides such a Poisson bracket⁴⁰ (with further relations, between the conjugate variables that are not relevant here).

Although no clear consensus has, in fact, emerged on the properties of Poisson bracket of rank-2 tensors⁴¹, if one focuses on the special case of strain tensors, that depend only on time, the following conjugate momentum can be introduced

$$\pi_{IJ} \equiv \frac{\partial \mathcal{L}}{\partial \dot{\epsilon}_{IJ}}, \quad (9)$$

where $\mathcal{L}(\epsilon_{IJ}(t), \dot{\epsilon}_{IJ}(t))$ is the unconstrained and free Lagrangian. $\dot{\epsilon}_{IJ}(t)$ are the components of the strain-rate tensor⁴².

Thus, we can build the corresponding Hamiltonian \mathcal{H} for the time evolution with tensor variables for mechanical deformations ϵ and their conjugated momenta π as the corresponding Legendre transform

$$\mathcal{H}(\epsilon, \pi) = \pi_{IJ} \dot{\epsilon}_{IJ} - \mathcal{L}, \quad (10)$$

up to a total time derivative for \mathcal{L} .

For the mechanical system only (i.e. for functions $A(\epsilon, \pi)$ and $B(\epsilon, \pi)$), the Poisson bracket can be defined in perfect analogy to that of any particle system, that explores a given target space geometry (to which refer the indices I, J, K, L), by the usual relations

$$\{A, B\}_{PB} = \frac{\partial A}{\partial \epsilon_{IJ}} \frac{\partial B}{\partial \pi_{IJ}} - \frac{\partial A}{\partial \pi_{IJ}} \frac{\partial B}{\partial \epsilon_{IJ}}. \quad (11)$$

In our case, the dynamical variables are the real symmetric rank-two tensors, ϵ_{IJ} and π_{IJ} ($I, J = 1, 2, 3$), which are canonically conjugate in the sense that their Poisson brackets are deemed to satisfy the following properties:

$$\{\epsilon_{IJ}, \pi_{KL}\}_{PB} = \delta_{IJKL}, \quad (12)$$

$$\{\epsilon_{IJ}, \epsilon_{KL}\}_{PB} = \{\pi_{IJ}, \pi_{KL}\}_{PB} = 0 \quad (13)$$

where δ_{IJKL} is a δ “tensor”, reflecting the real, symmetric, nature of the Poisson brackets⁴³ and defined as a product of Kronecker δ s. Very schematically, we may write

$$\delta_{IJKL} = \begin{cases} \delta_{IJ} \delta_{KL} \\ \delta_{IJ} \delta_{LK} \\ \delta_{JI} \delta_{LK} \\ \delta_{JI} \delta_{KL} \end{cases} \quad (14)$$

where each choice of the RHS corresponds to a choice of indices in the Poisson brackets. This choice can be supplemented by any linear combination of these δ s that enforces the symmetries of the tensors.

We now wish to include as phase space coordinates, the components of the spin vector, \mathbf{S} . We follow reference⁴⁴ and the details are summarized in appendix A. The “generalized” Poisson bracket, for the canonical variables of our system, can be written as

$$\{A, B\}_{PB} \equiv \frac{\partial A}{\partial \epsilon_{IJ}} \frac{\partial B}{\partial \pi_{IJ}} - \frac{\partial A}{\partial \pi_{IJ}} \frac{\partial B}{\partial \epsilon_{IJ}} - \frac{1}{\hbar} \epsilon_{IJK} S_I \frac{\partial A}{\partial S_J} \frac{\partial B}{\partial S_K}, \quad (15)$$

where \hbar is introduced to restore the physical dimensions of the Poisson bracket, since \mathbf{S} is dimensionless.

It should be stressed that this \hbar does not imply that any *quantum* effects are present, since the dynamics is fully classical. It is simply a bookkeeping device for a quantity that has the dimensions of angular momentum—i.e. of an area in phase space—and reflects the fact that the equation of motion for S_I is of first order. Quantum fluctuations will introduce the “real” \hbar .

Using this Poisson bracket, we can obtain the equations of motion for the phase space variables:

$$\begin{aligned}\dot{\varepsilon}_{IJ} &= \{\varepsilon_{IJ}, \mathcal{H}\}_{PB} = \frac{\partial \mathcal{H}}{\partial \pi_{IJ}} \\ \dot{\pi}_{IJ} &= \{\pi_{IJ}, \mathcal{H}\}_{PB} = -\frac{\partial \mathcal{H}}{\partial \varepsilon_{IJ}} \\ \dot{S}_I &= \{S_I, \mathcal{H}\}_{PB} = \frac{1}{\hbar} \varepsilon_{IJK} S_J \frac{\partial \mathcal{H}}{\partial S_K}\end{aligned}\quad (16)$$

The consistency of this formalism can be checked by noting that these equations preserve the volume in phase space

$$\frac{\partial \dot{\varepsilon}_{IJ}}{\partial \varepsilon_{IJ}} + \frac{\partial \dot{\pi}_{IJ}}{\partial \pi_{IJ}} + \frac{\partial \dot{S}_K}{\partial S_K} = 0. \quad (17)$$

That the dynamics preserves the volume in phase space does not, of course, imply anything about whether the system thus defined is integrable or shows Hamiltonian chaos.

The internal energy U , involving the mechanical energy for the deformed elastic medium²³, the magnetic energy, defined by the Zeeman term⁴⁵ and the magneto-elastic energy⁸, that takes into account the interaction of the magnetic moment with the medium, takes the form

$$\begin{aligned}U &= \frac{V_0}{2} C_{IJKL} \varepsilon_{IJ} \varepsilon_{KL} - V_0 \sigma_{IJ}^{\text{ext}} \varepsilon_{IJ} + B_{IJKL} \varepsilon_{IJ} S_K S_L \\ &\quad - \hbar \omega_I S_I,\end{aligned}\quad (18)$$

where C is the fully symmetric tensor, defining the elastic response, σ^{ext} is the external stress tensor, ω is the effective external magnetic field (expressed as a frequency) and B is the fully symmetric magnetostriction tensor.

The “kinetic” term, containing the conjugate momenta, can be written, schematically, as

$$\mathcal{H}_{\text{kinetic}} = \frac{1}{2} \pi_{IJ} M_{IJKL}^{-1} \pi_{KL} \quad (19)$$

where M is a fully symmetric “mass” matrix, that describes the inertial response.

For the case of isotropic materials, it is assuming that the M tensor has the form given by Lamé, with only two characteristic constants:

$$M_{IJKL} = M_0 \delta_{IJ} \delta_{KL} + M_1 (\delta_{IK} \delta_{JL} + \delta_{IL} \delta_{JK}). \quad (20)$$

The tensors C and B are decomposed in the same way.

Consequently, the inverse of these tensors can then be deduced from $M_{IJKL} M_{IJMN}^{-1} = \frac{1}{2} (\delta_{KM} \delta_{LN} + \delta_{KN} \delta_{LM})$. Thus

$$\begin{aligned}M_{IJKL}^{-1} &= \frac{-M_0}{2M_1(3M_0 + 2M_1)} \delta_{IJ} \delta_{KL} \\ &\quad + \frac{1}{4M_1} (\delta_{IK} \delta_{JL} + \delta_{IL} \delta_{JK})\end{aligned}\quad (21)$$

and the equations of motion become

$$\begin{cases} \dot{\varepsilon}_{IJ} = M_{IJKL}^{-1} \pi_{KL} \\ \dot{\pi}_{IJ} = -V_0 C_{IJKL} \varepsilon_{KL} + V_0 \sigma_{IJ}^{\text{ext}} - B_{IJKL} S_K S_L \\ \dot{S}_I = \varepsilon_{IJK} (\omega_J - \frac{2}{\hbar} B_{ABJC} \varepsilon_{AB} S_C) S_K \end{cases} \quad (22)$$

highlighting how the mechanical and magnetic subsystems are coupled.

The last equation—as expected!—is a precession equation for the components of \mathbf{S} around both the effective field ω and an additional field, that depends on the strain tensor and the spin vector.

In the following section we shall show how to solve these equations, in a way that preserves the symmetries of the extended phase space.

@Stam Stopped at 26/05/2019

IV. GEOMETRIC INTEGRATION

Solving the coupled system of equations (22) is the next step.

Since, in the previous section, we have shown that these equations describe a volume preserving transformation of the enlarged phase space, encompassing elastic *and* spin variables, it is natural to rewrite them, in terms of the action of a Liouville operator. Therefore, we shall write eqs.(22) as

$$\begin{aligned}\dot{\varepsilon} &= \mathcal{L}_\varepsilon \varepsilon, \\ \dot{\pi} &= \mathcal{L}_\pi \pi, \\ \dot{\mathbf{S}} &= \mathcal{L}_S \mathbf{S}.\end{aligned}\quad (23)$$

where \mathcal{L} is the Liouville operator. This formulation allows us to implement, manifestly, time-reversible, area preserving algorithms, for solving these equations numerically.

The general scheme is as follows: Consider an arbitrary function f of the canonically conjugate variables of our many-body system. This function, $f(\varepsilon, \pi, \mathbf{S})$, depends on the time t implicitly; that is, through the dependence of $(\varepsilon, \pi, \mathbf{S})$ on t . The time derivative of f is \dot{f} such as

$$\begin{aligned}\dot{f} &= \dot{\varepsilon}_{IJ} \frac{\partial f}{\partial \varepsilon_{IJ}} + \dot{\pi}_{IJ} \frac{\partial f}{\partial \pi_{IJ}} + \dot{S}_I \frac{\partial f}{\partial S_I} \\ &\equiv \mathcal{L}f.\end{aligned}\quad (24)$$

The last line defines the (total) Liouville operator

$$\mathcal{L} = \dot{\epsilon}_{IJ} \frac{\partial}{\partial \epsilon_{IJ}} + \dot{\pi}_{IJ} \frac{\partial}{\partial \pi_{IJ}} + \dot{S}_I \frac{\partial}{\partial S_I}. \quad (25)$$

Equation (24) can be integrated formally as an initial value problem to obtain f at any time :

$$f(\boldsymbol{\epsilon}(t), \boldsymbol{\pi}(t), \mathbf{S}(t)) = e^{\mathcal{L}t} f(\boldsymbol{\epsilon}(0), \boldsymbol{\pi}(0), \mathbf{S}(0)). \quad (26)$$

It is not difficult to see that $\mathcal{L} = \mathcal{L}_\epsilon + \mathcal{L}_\pi + \mathcal{L}_S$. However, these single Liouville operators do not commute two-by-two, as the reader may easily check by computing $\mathcal{L}_u \mathcal{L}_v f - \mathcal{L}_v \mathcal{L}_u f \neq 0$ for any function f and any combination (u, v) of the individual Liouville operator $\mathcal{L}_\epsilon, \mathcal{L}_\pi, \mathcal{L}_S$. This means that

$$e^{\mathcal{L}t} = e^{\mathcal{L}_\epsilon t + \mathcal{L}_\pi t + \mathcal{L}_S t} \neq e^{\mathcal{L}_\epsilon t} e^{\mathcal{L}_\pi t} e^{\mathcal{L}_S t}. \quad (27)$$

According to the Magnus expansion⁴⁶, however, it is always possible to express $e^{\mathcal{L}t}$ as a product of the individual operators at any given order in time, according to the so-called ‘‘splitting method’’⁴⁷. This ensures that the numerical algorithm preserves phase space volumes exactly.

For instance, for a fixed timestep τ , upon expanding up to the third order in time, the following sequence of products

$$e^{\mathcal{L}\tau} = e^{\mathcal{L}_S \frac{\tau}{4}} e^{\mathcal{L}_\pi \frac{\tau}{2}} e^{\mathcal{L}_S \frac{\tau}{4}} e^{\mathcal{L}_\epsilon \tau} e^{\mathcal{L}_S \frac{\tau}{4}} e^{\mathcal{L}_\pi \frac{\tau}{2}} e^{\mathcal{L}_S \frac{\tau}{4}} + \mathcal{O}(\tau^3), \quad (28)$$

can be generated; this sequence is, in fact, one of six possible, that have the property of preserving the symplectic structure of the Poisson brackets. Therefore, any one of them can be chosen. The possible combinations are presented in table I. While these schemes are free from

A	$\frac{\tau}{4}$	$\frac{\tau}{2}$	$\frac{\tau}{4}$	τ	$\frac{\tau}{4}$	$\frac{\tau}{2}$	$\frac{\tau}{4}$
1	\mathbf{S}	$\boldsymbol{\pi}$	\mathbf{S}	$\boldsymbol{\epsilon}$	\mathbf{S}	$\boldsymbol{\pi}$	\mathbf{S}
2	\mathbf{S}	$\boldsymbol{\epsilon}$	\mathbf{S}	$\boldsymbol{\pi}$	\mathbf{S}	$\boldsymbol{\epsilon}$	\mathbf{S}
3	$\boldsymbol{\pi}$	$\boldsymbol{\epsilon}$	$\boldsymbol{\pi}$	\mathbf{S}	$\boldsymbol{\pi}$	$\boldsymbol{\epsilon}$	$\boldsymbol{\pi}$
4	$\boldsymbol{\pi}$	\mathbf{S}	$\boldsymbol{\pi}$	$\boldsymbol{\epsilon}$	$\boldsymbol{\pi}$	\mathbf{S}	$\boldsymbol{\pi}$
5	$\boldsymbol{\epsilon}$	$\boldsymbol{\pi}$	$\boldsymbol{\epsilon}$	\mathbf{S}	$\boldsymbol{\epsilon}$	$\boldsymbol{\pi}$	$\boldsymbol{\epsilon}$
6	$\boldsymbol{\epsilon}$	\mathbf{S}	$\boldsymbol{\epsilon}$	$\boldsymbol{\pi}$	$\boldsymbol{\epsilon}$	\mathbf{S}	$\boldsymbol{\epsilon}$

Table I. Decomposition table of symplectic integrators

‘‘global’’ errors, they are, of course, sensitive to ‘‘local’’ errors, due to the finite value of the timestep. It is, also, not at all obvious that all six can be implemented with comparable efficiency. It is, therefore, useful to study the numerical stability and efficiency of these different combinations, in particular, as former studies in molecular dynamics⁴⁸ and magnetic molecular dynamics¹² showed, apparently, numerical differences between them.

A sampler of such a study is presented in appendix B.

It is important to keep in mind that the one-step evolution operators for $\boldsymbol{\epsilon}$ and $\boldsymbol{\pi}$ describe shifts of the corresponding tensor components, whereas the one-step evolution operator for \mathbf{S} describes rotations. In equations

$$e^{\mathcal{L}_\epsilon \tau}(\boldsymbol{\epsilon}(t), \boldsymbol{\pi}(t), \mathbf{S}(t)) = (\boldsymbol{\epsilon}(t) + \tau \dot{\boldsymbol{\epsilon}}(t), \boldsymbol{\pi}(t), \mathbf{S}(t)) \quad (29)$$

$$e^{\mathcal{L}_\pi \tau}(\boldsymbol{\epsilon}(t), \boldsymbol{\pi}(t), \mathbf{S}(0)) = (\boldsymbol{\epsilon}(t), \boldsymbol{\pi}(t) + \tau \dot{\boldsymbol{\pi}}(t), \mathbf{S}(t)) \quad (30)$$

$$e^{\mathcal{L}_S \tau}(\boldsymbol{\epsilon}(t), \boldsymbol{\pi}(t), \mathbf{S}(t)) = (\boldsymbol{\epsilon}(t), \boldsymbol{\pi}(t), \underbrace{\mathbf{S}(t + \tau)}_{R(\tau)\mathbf{S}(t)}) \quad (31)$$

where $\mathbf{S}(t + \tau) = R(\tau)\mathbf{S}(t)$ is given by the Rodrigues’ rotation formula⁴⁹ for a spin vector around a given rotation vector $\tilde{\boldsymbol{\omega}}(t)$ where each of its components are $\tilde{\omega}_I(t) = \omega_I(t) - \frac{2}{\hbar} B_{JKLI} \epsilon_{JK}(t) S_L(t)$. These equations describe the phase space of one particle only. To describe the dynamics of a continuum, we must deduce the equations for many particles.

One way to generalize eqs.(22) for the case of many particles, labeled by an index, $i = 1, \dots, N$, according to the conventions of the previous sections, is the following

$$\dot{\epsilon}_{IJ}^i = [M^i]_{IJKL}^{-1} \pi_{KL}^i \quad (32)$$

$$\dot{\pi}_{IJ}^i = -V_0 C_{IJKL}^i \epsilon_{KL}^i + V_0 \sigma_{IJ}^{i \text{ ext}} - B_{IJKL}^i S_K^i S_L^i \quad (33)$$

$$\dot{S}_I^i = \epsilon_{IJK} \left(\omega_J^i - \frac{2}{\hbar} B_{ABJC}^i \epsilon_{AB}^i S_C^i \right) S_K^i \quad (34)$$

The case of a staggered AF state is treated simply by letting $N = 2$. In order to simplify the mechanical part further, we can impose additional conditions pertaining to the uniformity of the external stress, mechanical constants, mass matrices and magneto-elastic constants, at each site. In what follows, we shall use the following *Ansatz*:

$$\begin{aligned} B_{IJKL}^1 &= B_{IJKL}^2, \\ C_{IJKL}^1 &= C_{IJKL}^2, \\ M_{IJKL}^1 &= M_{IJKL}^2, \\ \sigma_{IJ}^{1 \text{ ext}} &= \sigma_{IJ}^{2 \text{ ext}}. \end{aligned} \quad (35)$$

The conservative part of the precession contains a local field, which is modified to include the antiferromagnetic exchange between the sites and a single anisotropy axis \mathbf{n} with an intensity K . One has

$$\omega_I^i = \frac{1}{\hbar} \sum_{\langle ij \rangle} J^{ij} S_I^j + \frac{K}{\hbar} n_J S_J^i n_I \quad (36)$$

Because of the exchange field, the Liouville operators for different spins do not commute either. A global geometric integrator, implementing the approach of Omelyan⁵⁰, which remains accurate up to third order in the timestep expansion must, therefore, be constructed.

For any given timestep, τ , the corresponding expression for the evolution operator, reads

$$e^{\mathcal{L}_S \tau} = e^{\mathcal{L}_{S^1} \frac{\tau}{2}} e^{\mathcal{L}_{S^2} \tau} e^{\mathcal{L}_{S^1} \frac{\tau}{2}} + \mathcal{O}(\tau^3). \quad (37)$$

For $N = 2$, this operator is numerically identical to the operator, obtained by permuting the site indices, $1 \leftrightarrow 2$.

The same reasoning is applied for the Liouville operators for the elastic variables, that enter in equations (23) and the corresponding global geometric integrators are constructed along the same lines. The system is then integrated by following one of the schemes displayed in table I.

With these tools, we can study a plethora of phenomena, that are sensitive to the coupling of magnetic, electric and elastic degrees of freedom. In the following section we shall apply this formalism for studying “switching” effects of the magnetization in antiferromagnetic media. The numerical accuracy ensured by the geometric integrators is necessary to describe picosecond switching times.

V. ANTIFERROMAGNETIC ULTRAFAST SWITCHING UNDER STRESS

In this section, we shall apply the formalism constructed above, to describe how it is possible to generate and manipulate picosecond switching of the magnetization, induced by STTs, from a short pulse of electric current, in elastic media that exhibit staggered AF order. Such a fast switching process in AFs is schematically

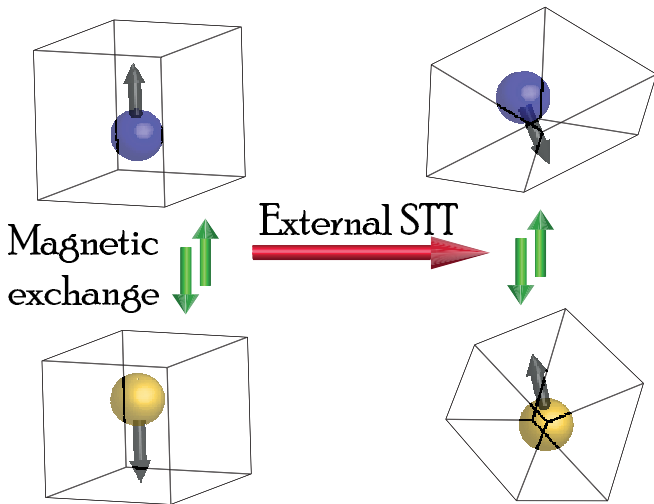


Figure 1. (Color online) Switching scheme for antiferromagnetic magneto-mechanically coupled toy model with external STT.

displayed in figure 1 and can be realized, in practice, by a femtosecond laser excitation of the magnetic moments that generate a field-induced STT on the two sub-lattices. During the pulse, energy is transferred from conduction electrons to the sub-lattice magnetic moments via STT (this is how the electric current affects the magnetic response), and hence contributes to the exchange energy between the moments, since local moments can be canted noncollinearly. The energy due to the strong ex-

change interaction between neighboring moments, which is commonly found in AFs, in particular due to magnetic anisotropy, appears as an effective inertia to the motion, leading to the appearance of a time scale, much longer than that of the excitation pulse. Afterwards, the system follows a natural path along the easy-plane to circumvent the unfavorable anisotropy barrier and finally relaxes to a new magnetic configuration. The resulting dynamics is a switching of the two sub-lattices moments to the opposite direction through the easy-plane.

This process defines the ultrafast antiferromagnetic switching effect.

During the process, the Néel vector, that probes the difference between the magnetic moments of the two sub-lattices, acquires a net value that can be transferred as a so-called “spin accumulation”, to an adjacent non-magnetic normal material in order to pump the produced spin current via scattering of electrons. The reverse mechanism can be realized, as well.

What was not considered before is the possibility to enhance or inhibit such a switching, depending on tensile or compression effects, that are generated by an external stress, that couples to the internal strain, produced by the intrinsic magneto-elastic interaction in such materials, as depicted in figure 1.

In order to conform to the notation used in our previous studies²², equation (34) is supplemented with a non-conservative part, labeled \mathbf{T} , on the RHS, which includes both a transverse damping and a field-like STT torque

$$T_I^i = \alpha \epsilon_{IJK} S_J^i \dot{S}_K^i + G (s_I^i s_J^i p_J - p_I s_J^i s_J^i). \quad (38)$$

The resulting equations of motion, are numerically integrated, using the approach of section V. It is noteworthy that, this equation, also, describes the “backreaction” of the magnetic response on the spin transfer torque. On the other hand, we do not consider how this backreaction affects the current pulse itself, that’s assumed external.

In figures 2 and 3 we report the evolution of the average magnetization $\mathbf{m} \equiv \frac{1}{2} (\mathbf{S}^1 + \mathbf{S}^2)$ and the Néel vector $\mathbf{l} \equiv \frac{1}{2} (\mathbf{S}^1 - \mathbf{S}^2)$, in the presence as well as the absence of magnetoelastic coupling, for a moderate external isotropic stress of $30\mu_0 M_s^2$. The conditions and values of the simulation are identical to those found by Cheng *et al.*²¹. We start the simulations using an initial configuration, where spins are aligned along the \hat{x} -axis in an antiferromagnetic configuration and apply two 10 ps electric pulses of 0.0034 rad.THz intensity, each separated by 50 ps, in the $\mathbf{p} = \hat{z}$ -direction. In addition to the exchange interaction, the spins are subjected to a global anisotropy, along the $\mathbf{n} = \hat{x}$ -axis.

In the absence of magnetoelastic coupling, our results are identical to those by Cheng *et al.*²¹ and to those we obtained under the same conditions in our previous work²².

In the presence of magnetoelastic coupling, however, as the mechanical system is undamped, the results are quite different. In figure 4 we display the evolution of the strain components over time.

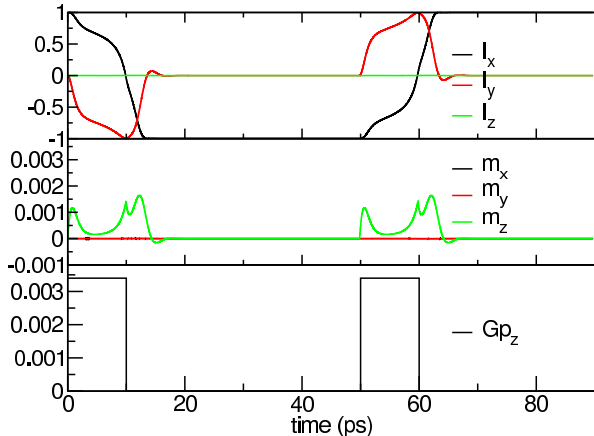


Figure 2. (Color online) Average magnetization (upper panel) and Néel order parameter components (middle panel) for uncoupled switching with parameters in reference²². The lower panel displays the STT pulses. The figures agree with the reference²¹ because the magnetoelastic constants are set to zero.

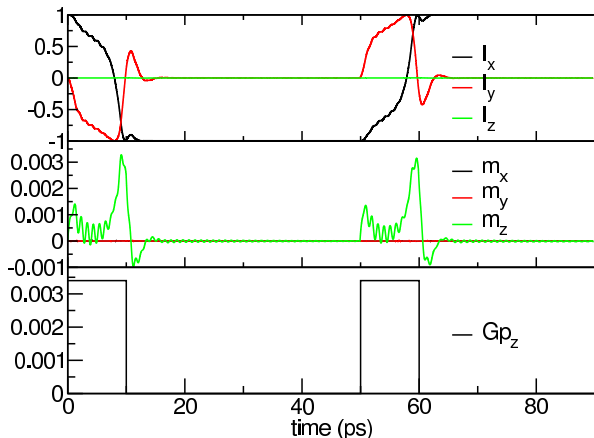


Figure 3. (Color online) Average magnetization (upper panel) and Néel order parameter components (middle panel) for a coupled switching with parameters in reference²². The lower panel displays the STT pulses. Here $B_0 = 7.7\mu_0 M_s^2$ and $B_1 = -23\mu_0 M_s^2$.

Because of the presence of a constant stress, a finite mass matrix and non-zero elastic constants, the mechanical system is expected to be oscillating freely, which is, indeed, observed.

These oscillations are also observed, both in the magnetization and the Néel vector in the figure 3, in the form of small wiggles, superimposed on the main component of the spin accumulation vector. A compression in one direction becomes tensile in the other one and vice-versa because of the sign of B_1 . As a consequence

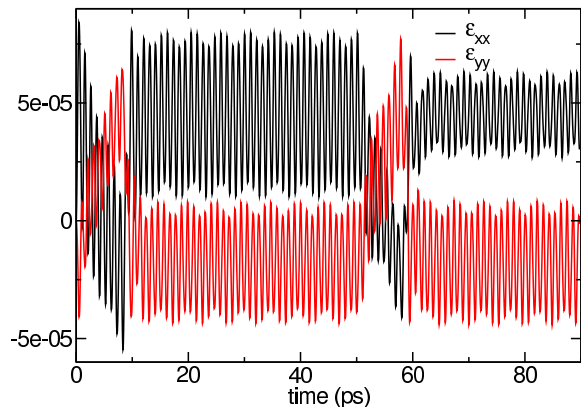


Figure 4. (Color online) Strain components as a function of time with the magnetoelastic constants turned on with parameters in reference²².

of such a mechanical deformation, the switching time of the magnetization is slightly faster and the amplitude of the magnetization enhanced, depending on the value of the stress and magnetoelastic constants, as observed in figure 3. On the other hand, the strain tensor itself is quasi-uniform in space on the two sub-lattices.

VI. DISCUSSION

In the previous sections, we have described how to realize a mechanism for the ultrafast switching of the magnetization, that can be induced by a STT in NiO, where both the duration and intensity can be modulated by appropriate internal strain, thanks to magnetoelastic coupling. Such a strain can be modulated, in return, by the induced magnetization process by the same magnetoelastic coupling in order to produce a modulated elastic wave. Depending on the pulse duration and transverse damping value, the terminal angle of the Néel vector evolves gradually by integer values of π as already shown²¹. In real experiments, because amplitude fluctuations of the electric pulses are inevitable, small damping values are not favorable since it may easily lead to overshoot, which is amplified by the mechanical response. When Joule heating in the normal underlying metal is taken into account, a shorter pulse with stronger current intensity should be desirable, but a modulated undamped mechanical strain is then produced. For the moment, what is not easy to predict are the mechanical damping mechanisms induced by a differential thermal stress produced by such a Joule heating, where its effect superimposes to the whole dynamics. However, at least for the case of undamped dynamics, we have developed the mathematical and computational framework, that consistently takes into account elastic and magnetic degrees of freedom and that pro-

vides a starting point for designing future AFs devices for spintronics applications that combine both mechanical and magnetic coupled responses.

ACKNOWLEDGMENTS

All authors contributed equally to the manuscript. T.N. acknowledges financial support through a joint doctoral fellowship ‘‘CEA–Région Centre’’ under grant number 201600110872.

Appendix A: A model for precession through anticommuting variables

We review some issues when dealing with classical spin variables and explain some limitations which are met by using the framework of commuting variables^{51,52}. A common starting point to build precessional models is choosing the appropriate representation of the $\mathfrak{su}(2)$ algebra.

In the Heisenberg picture the Ehrenfest theorem implies that the equations of motion for the average of the spin operator $\hat{\mathbf{S}}$ components read

$$i\hbar \frac{d\langle \hat{\mathbf{S}} \rangle}{dt} = \langle [\hat{\mathbf{S}}, \mathcal{H}] \rangle \quad (\text{A1})$$

where \mathcal{H} is the Zeeman Hamiltonian operator for an external magnetic field \mathbf{H} such that

$$\mathcal{H} = -g\mu_0\mu_B \hat{\mathbf{S}} \cdot \mathbf{H}. \quad (\text{A2})$$

From the commutation relations $[\hat{S}_i, \hat{S}_j] = i\epsilon_{ijk}\hat{S}_k$, one can quite straightforwardly show that

$$\frac{d\langle \hat{\mathbf{S}} \rangle}{dt} = \frac{g\mu_B\mu_0}{\hbar} \langle \hat{\mathbf{S}} \rangle \times \mathbf{H}, \quad (\text{A3})$$

which corresponds to the well-known Larmor precession of the expectation value of the spin in an external magnetic field \mathbf{H} .

Interestingly, a different–but equivalent–approach can be followed, by considering the Majorana representation, in terms of anticommuting variables, ξ_I , $\xi_I\xi_J + \xi_J\xi_I = 0$ ³¹ of the vector \mathbf{S} :

$$S_I = -\frac{i}{2}\epsilon_{IJK}\xi_J\xi_K, \quad (\text{A4})$$

which can easily be shown to commute, as $S_I S_J = 0$. This last relation is, of course, not satisfactory. It can be easily avoided, however, by imposing that the ξ_I satisfy the anticommutation relations $\{\xi_I, \xi_J\} = \delta^{ij}$ –that they generate a Clifford algebra (up to a constant normalization)³².

These relations imply that the S_I define a spin–1/2 representation of the $\mathfrak{su}(2)$ algebra. Higher spin representations can be defined by multilinear combinations²⁰, that are relevant for describing magnetic properties of

composite objects; since we can work with the S_I instead of the ξ_I , however, this complication will not affect us here.

This representation highlights that the spin degrees of freedom, S_I , are, in fact, ‘‘composite’’ objects and that the ‘‘fundamental degrees of freedom’’ are the ξ_I . Therefore, it is useful to develop the description of the dynamics, directly, in terms of the ξ_I themselves. We shall recall the salient features below.

The Poisson brackets for the anticommuting variables ξ_I are related to those of S_I , in order that the dynamics be, indeed, equivalent, in a way that was set forth many years ago, through the construction of a corresponding graded Poisson bracket, which generalizes Poisson brackets from manifolds to super-manifolds¹⁸.

In terms of any functions of anti-commuting variables ξ this bracket reads

$$\{f(\xi), g(\xi)\}_{\text{PB}} \equiv \frac{i}{\hbar} f(\xi) \overleftarrow{\frac{\partial}{\partial \xi_K}} \overrightarrow{\frac{\partial}{\partial \xi_K}} g(\xi), \quad (\text{A5})$$

with the corresponding definition of the left and right derivative of any function of the anti-commuting variables. One can show that this bracket, also known as the ‘‘antibracket’’ of any two functions on a flat super-manifold, satisfies all necessary properties for a graded bracket, namely (graded) Leibniz rule, (graded) antisymmetry and (graded) Jacobi identity⁵³.

By taking this graded Poisson bracket for any two of these anti-commuting variables, we get

$$\{\xi_I, \xi_J\}_{\text{PB}} = \frac{i}{\hbar} \delta_{IJ}. \quad (\text{A6})$$

This implies that any two such variables are canonically conjugate, since $\{\xi_I, -i\hbar\xi_J\}_{\text{PB}} = \delta_{IJ}$ and $\pi_I \equiv -i\hbar\xi_I$ defines the canonical conjugate^{19,20}.

By using the Grassmann properties of ξ , one proves that

$$\{S_I, S_J\}_{\text{PB}} = \frac{1}{\hbar} \epsilon_{IJK} S_K \quad (\text{A7})$$

which is a consistency check that the S_I as defined in (A4) do realize a representation of the rotation group.

In eq.(A5), if the functions of the ξ are chosen to contain only quadratic terms, then one can identify the previous bracket as a regular Poisson bracket on a Riemannian manifold for the commuting variables \mathbf{S}

$$\begin{aligned} \{f(\mathbf{S}), g(\mathbf{S})\}_{\text{PB}} &= \frac{i}{\hbar} \frac{\partial f}{\partial S_I} S_I \overleftarrow{\frac{\partial}{\partial \xi_K}} \overrightarrow{\frac{\partial}{\partial \xi_K}} S_J \frac{\partial g}{\partial S_J} \\ &= \{S_I, S_J\}_{\text{PB}} \frac{\partial f}{\partial S_I} \frac{\partial g}{\partial S_J} = \frac{1}{\hbar} \epsilon_{IJK} S_K \frac{\partial f}{\partial S_I} \frac{\partial g}{\partial S_J}, \end{aligned} \quad (\text{A8})$$

which is, precisely, the ‘‘spinning part’’ of the bracket introduced by Yang and Hirschfelder⁴⁴ for magnetized fluid dynamics, which reads as

$$\{A, B\}_{\text{PB}} \equiv \frac{\partial A}{\partial q_I} \frac{\partial B}{\partial p_I} - \frac{\partial A}{\partial p_I} \frac{\partial B}{\partial q_I} - \frac{1}{\hbar} \epsilon_{IJK} S_I \frac{\partial A}{\partial S_J} \frac{\partial B}{\partial S_K}. \quad (\text{A9})$$

Similar expressions have been found already by Casalbuoni a long time ago¹⁹ without having attracted the attention they deserve. Following the inverse path of canonical quantization, we use this graded Poisson Bracket on any commuting quantity, which allows us to compute directly

$$\{\mathbf{S}, \mathcal{H}\}_{PB} = \frac{g\mu_B\mu_0}{\hbar} \mathbf{S} \times \mathbf{H} \quad (\text{A10})$$

thereby highlighting that the description of \mathbf{S} in terms of $\boldsymbol{\xi}$ is an equivalent description of the dynamics.

For any time-dependent commuting functions of $\mathbf{S}(t)$, we can use this Poisson bracket to deduce a Liouville equation

$$\frac{dF(\mathbf{S}(t))}{dt} = \{F(\mathbf{S}(t)), \mathcal{H}\}_{PB}. \quad (\text{A11})$$

Consequently, the equations of motion for the variables $\boldsymbol{\xi}$ read much more simple expressions as

$$\frac{d\boldsymbol{\xi}(t)}{dt} = \{\boldsymbol{\xi}, \mathcal{H}\}_{PB} = \frac{i}{\hbar} \frac{\overrightarrow{\partial} \mathcal{H}}{\partial \boldsymbol{\xi}}, \quad (\text{A12})$$

which are known to form a non-relativistic pseudoclassical mechanics¹⁹.

One reason why using the representation of \mathbf{S} in terms of $\boldsymbol{\xi}$ is useful is that it is intrinsically difficult to build a Lagrangian model for the commuting spin variable \mathbf{S} , since its canonically conjugate variable cannot be unambiguously identified. As is, by now, well known, the conjugate of the dynamical variable $\boldsymbol{\xi}$ is proportional to itself⁵⁴. Therefore, the dynamics of spinning degrees of freedom can be described, either through a vector of commuting variables on a curved manifold, or by a vector of anti-commuting variables on a flat—though non-Riemannian—manifold. Finally, it has been found that the Majorana-fermion representation of 1/2-spin operators is also a powerful tool to straightforwardly compute spin-spin correlators⁵⁵, which represents an advantage for computing magnetic response functions in a many-bodies formulation.

Appendix B: Numerical accuracy of the splitting algorithms

The accuracy of the numerical schemes represented in table I depends on the relative amplitude of the velocity terms ($\dot{\epsilon}, \dot{\pi}, \dot{S}$), and can be monitored by checking the stability of equation (17) over time^{46,47}.

Figure 5 displays the total energy in one domain (given by the sum of eqs.(18) and (19)) upon varying the numerical precision. The splitting algorithm considered corresponds to the label $A = 1$ in table I. The numerical precision is controlled by the “quality factor Q ”, chosen

at the beginning of the simulation, which produces variable timesteps τ according to the relation $\tau = Q/\|\omega\|$.

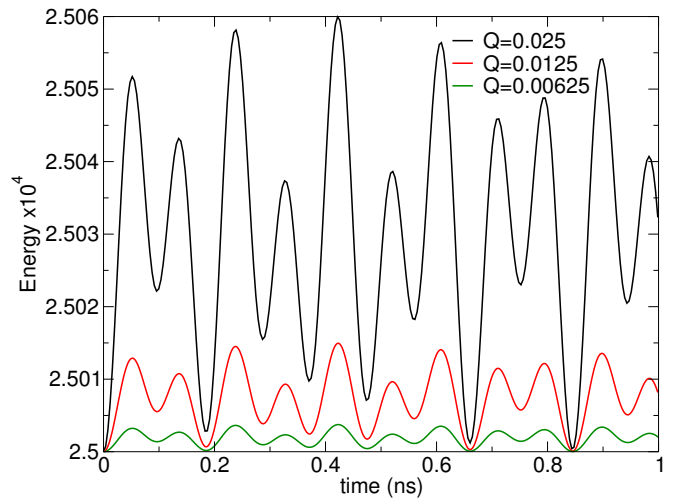


Figure 5. (Color online) Single-site total energy as a function of both time and variable timestep Q . Conditions of the simulation are expressed in reduced units: $2C_0/\mu_0 M_s^2 = 5.1 \times 10^5$, $2C_1/\mu_0 M_s^2 = 3.5 \times 10^5$, $M_1 V_0 \mu_0 M_s^2 / 2\hbar^2 = 1000$, $\omega_{DC} = (0, 0, 2\pi)$ rad.GHZ, $\pi_{11}(0) = 1$, $\mathbf{s}(0) = (1, 0, 0)$. All the other parameters not reported, included initial conditions are zero.

$\pi_{11}^2(0)/4M_1$, which has to stay constant over time. We observe that this is, indeed, the case, whatever the value of the quality factor Q . We remark that, as $Q \rightarrow 0$, the variations about the average value of the energy are suppressed, as should be expected.

Figure 6 displays some of the non-vanishing components of the strain tensor over time (here $\epsilon_{22}(t) = \epsilon_{33}(t)$ and this third component is not reported), when using different splitting algorithms, among those displayed in Table I. We observe less than 1% of numerical relative difference between the two algorithms on the strain and its conjugate variables, and no difference (up to the machine precision) on the magnetization with a “coarse” quality factor Q , which cannot be detected by visual inspection on the figure. This difference falls to 0.1% when the quality factor is divided by 4. The same procedure can be repeated for all the splitting combinations in Table I, the conclusions previously drawn apply, also, for the magnetization, strain and its conjugate variable, depending on the frequency of appearance of the splitted operator. As expected, once a splitting algorithm is selected, the more frequently an operator is evaluated, the smaller the error, though, of course, the time required, also, grows. This opens the possibility to select optimally a proper splitting algorithm, depending on the relative intensity of $\dot{\epsilon}_{ij}, \dot{\pi}_{ij}, \dot{S}_i$ over time.

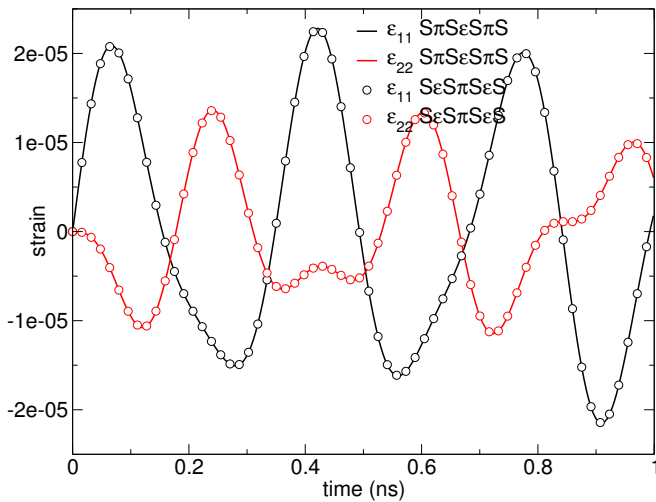


Figure 6. (Color online) Single-site strain components as a function of time for various numerical schemes. Conditions of the simulation are identical to those for figure 5 and the results are produced for $Q = 0.0025$ only.

-
- * thomas.nussle@cea.fr
† pascal.thibaudeau@cea.fr
‡ stam.nicolis@lmpt.univ-tours.fr
- ¹ J. H. Lee, L. Fang, E. Vlahos, X. Ke, Y. W. Jung, L. F. Kourkoutis, J.-W. Kim, P. J. Ryan, T. Heeg, M. Roeckerath, V. Goian, M. Bernhagen, R. Uecker, P. C. Hammel, K. M. Rabe, S. Kamba, J. Schubert, J. W. Freeland, D. A. Muller, C. J. Fennie, P. Schiffer, V. Gopalan, E. Johnston-Halperin, and D. G. Schlom, *Nature* **466**, 954 (2010).
 - ² I. Radu, K. Vahaplar, C. Stamm, T. Kachel, N. Pontius, H. Dürr, T. Ostler, J. Barker, R. Evans, R. Chantrell, *et al.*, *Nature* **472**, 205 (2011); T. Jungwirth, X. Marti, P. Wadley, and J. Wunderlich, *Nature Nanotechnology* **11**, 231 (2016).
 - ³ J. Železný, P. Wadley, K. Olejník, A. Hoffmann, and H. Ohno, *Nature Physics* **14**, 220 (2018).
 - ⁴ H. Ahmad, J. Atulasimha, and S. Bandyopadhyay, *Scientific Reports* **5**, 18264 (2015).
 - ⁵ H. Yan, Z. Feng, S. Shang, X. Wang, Z. Hu, J. Wang, Z. Zhu, H. Wang, Z. Chen, H. Hua, W. Lu, J. Wang, P. Qin, H. Guo, X. Zhou, Z. Leng, Z. Liu, C. Jiang, M. Coey, and Z. Liu, *Nature Nanotechnology* **14**, 131 (2019).
 - ⁶ M. Fiebig, *Journal of Physics D: Applied Physics* **38**, R123 (2005).
 - ⁷ J. Atulasimha and S. Bandyopadhyay, *Applied Physics Letters* **97**, 173105 (2010).
 - ⁸ E. Du Trémolet de Lacheisserie, *Magnetostriction: Theory and Applications of Magnetoelasticity* (CRC Press, Boca Raton, 1993).
 - ⁹ P. Bruno, *Physical Review B* **39**, 865 (1989).
 - ¹⁰ P. Bruno, in *Ferienkurse Des Forschungszentrums Jülich* (Jülich, 1993).
 - ¹¹ D. I. Bardzokas, M. L. Filstinsky, and L. A. Filstinsky, *Mathematical Methods in Electro-Magneto-Elasticity*, Lecture Notes in Applied and Computational Mechanics, Vol. 32 (Springer Berlin Heidelberg, Berlin, Heidelberg, 2007).
 - ¹² D. Beaujouan, P. Thibaudeau, and C. Barreteau, *Physical Review B* **86**, 174409 (2012).
 - ¹³ E. DeGiuli, *Physical Review E* **98**, 033001 (2018), arXiv:1804.04834.
 - ¹⁴ G. A. Maugin, *Continuum Mechanics of Electromagnetic Solids*, North Holland Series in Applied Mathematics and Mechanics No. 33 (North Holland, Amsterdam, 1988).
 - ¹⁵ N. Buiron, L. Hirsinger, and R. Billardon, *Le Journal de Physique IV* **09**, Pr9 (1999).
 - ¹⁶ L. Daniel and N. Galopin, *The European Physical Journal Applied Physics* **42**, 153 (2008).
 - ¹⁷ C. C. Mei and B. Vernescu, *Homogenization Methods for Multiscale Mechanics* (World Scientific, Singapore, 2010).
 - ¹⁸ R. Casalbuoni, *Il Nuovo Cimento A (1965-1970)* **33**, 115 (1976).
 - ¹⁹ R. Casalbuoni, *Il Nuovo Cimento A (1965-1970)* **33**, 389 (1976).
 - ²⁰ F. Berezin and M. Marinov, *Annals of Physics* **104**, 336 (1977).
 - ²¹ R. Cheng, M. W. Daniels, J.-G. Zhu, and D. Xiao, *Physical Review B* **91**, 064423 (2015).
 - ²² T. Nussle, P. Thibaudeau, and S. Nicolis, *Journal of Magnetism and Magnetic Materials* **469**, 633 (2019), arXiv:1711.08062.
 - ²³ L. D. Landau, E. M. Lifshitz, and L. D. Landau, *Theory of Elasticity*, 3rd ed., Course of Theoretical Physics No. Vol. 7 (Elsevier, Amsterdam, 2008).
 - ²⁴ B. K. D. Gairola, *Physica Status Solidi (b)* **85**, 577 (1978).
 - ²⁵ A. C. Eringen, ed., *Nonlocal Continuum Field Theories* (Springer New York, New York, NY, 2004).
 - ²⁶ R. A. Toupin and B. Bernstein, *The Journal of the Acoustical Society of America* **33**, 216 (1961); E. R. Callen and H. B. Callen, *Physical Review* **129**, 578 (1963); W. F. Brown, *Magnetoelastic Interactions*, edited by C. Trues-

- dell, R. Aris, L. Collatz, G. Fichera, P. Germain, J. Keller, M. M. Schiffer, and A. Seeger, Springer Tracts in Natural Philosophy, Vol. 9 (Springer Berlin Heidelberg, Berlin, Heidelberg, 1966).
- ²⁷ G. Rosen, American Journal of Physics **40**, 683 (1972).
- ²⁸ H. F. Tiersten, Journal of Mathematical Physics **5**, 1298 (1964); A. Akhiezer, V. Bar'yakhtar, and S. Peletminskii, *Spin Waves*, North Holland Series in Low Temperature Physics, Vol. 1 (Amsterdam, 1968).
- ²⁹ D. Dever, Journal of Applied Physics **43**, 3293 (1972).
- ³⁰ F. Wilczek, Nature Physics **5**, 614 (2009).
- ³¹ J. Alicea, Reports on Progress in Physics **75**, 076501 (2012).
- ³² P. Lounesto, *Clifford Algebras and Spinors*, 2nd ed., London Mathematical Society Lecture Note Series No. 286 (Cambridge Univ. Press, Cambridge, 2003).
- ³³ R. F. Evans, W. J. Fan, P. Chureemart, T. A. Ostler, M. O. Ellis, and R. W. Chantrell, Journal of Physics: Condensed Matter **26**, 103202 (2014).
- ³⁴ O. Eriksson, A. Bergman, L. Bergqvist, and J. Hellsvik, *Atomistic Spin Dynamics: Foundations and Applications*, first edition ed. (Oxford University Press, Oxford, 2017).
- ³⁵ J. H. van Vleck, Physical Review **52**, 1178 (1937).
- ³⁶ L. Néel, Journal de Physique et le Radium **15**, 225 (1954).
- ³⁷ E. W. Lee, Reports on Progress in Physics **18**, 184 (1955).
- ³⁸ R. F. Sabiryanov and S. S. Jaswal, Physical Review Letters **83**, 2062 (1999).
- ³⁹ H. A. Kastrup, Physics Reports **101**, 1 (1983); I. V. Kanatchikov, arXiv:9312162 (hep-th) (1993).
- ⁴⁰ R. Arnowitt, S. Deser, and C. W. Misner, Physical Review **117**, 1595 (1960).
- ⁴¹ S. A. Hojman, K. Kuchař, and C. Teitelboim, Annals of Physics **96**, 88 (1976).
- ⁴² R. Hill, Proceedings of the Royal Society of London. A. Mathematical and Physical Sciences **314**, 457 (1970).
- ⁴³ J. Kijowski and W. Szczyrba, Communications in Mathematical Physics **46**, 183 (1976); W. Szczyrba, *ibid.* **51**, 163 (1976); J. E. Marsden, R. Montgomery, P. J. Morrison, and W. B. Thompson, Annals of Physics **169**, 29 (1986).
- ⁴⁴ K.-H. Yang and J. O. Hirschfelder, Physical Review A **22**, 1814 (1980).
- ⁴⁵ R. Skomski, *Simple Models of Magnetism*, Oxford Graduate Texts (Oxford University Press, Oxford, New York, 2008).
- ⁴⁶ S. Blanes, F. Casas, J. A. Oteo, and J. Ros, Physics Reports **470**, 151 (2009).
- ⁴⁷ E. Hairer, C. Lubich, and G. Wanner, *Geometric Numerical Integration: Structure-Preserving Algorithms for Ordinary Differential Equations*, 2nd ed., Springer Series in Computational Mathematics (Springer-Verlag, Berlin Heidelberg, 2006).
- ⁴⁸ P. F. Batcho and T. Schlick, The Journal of Chemical Physics **115**, 4019 (2001).
- ⁴⁹ O. Rodrigues, Journal de Mathématiques Pures et Appliquées **5**, 380 (1840); J. Honerkamp and H. Römer, *Theoretical Physics: A Classical Approach* (Springer, Berlin; New York, 1993); P. Thibaudeau and D. Beaujouan, Physica A: Statistical Mechanics and its Applications **391**, 1963 (2012).
- ⁵⁰ I. P. Omelyan, I. M. Mryglod, and R. Folk, Computer Physics Communications **151**, 272 (2003).
- ⁵¹ L. Brink, P. Di Vecchia, and P. Howe, Physics Letters B **65**, 471 (1976).
- ⁵² L. Brink, P. Di Vecchia, and P. Howe, Nuclear Physics B **118**, 76 (1977).
- ⁵³ J. Gomis, J. París, and S. Samuel, Physics Reports **259**, 1 (1995); I. V. Kanatchikov, Reports on Mathematical Physics **40**, 225 (1997).
- ⁵⁴ R. Casalbuoni, Physics Letters B **62**, 49 (1976).
- ⁵⁵ A. Shnirman and Y. Makhlin, Physical Review Letters **91**, 207204 (2003); W. Mao, P. Coleman, C. Hooley, and D. Langreth, *ibid.* **91**, 207203 (2003); P. Schad, Y. Makhlin, B. N. Narozhny, G. Schön, and A. Shnirman, Annals of Physics **361**, 401 (2015).